PHYSICAL REVIEW D **84,** 053008 (2011)

Sterile neutrino mixing with ν_τ

Juan Carlos Helo, Sergey Kovalenko, and Ivan Schmidt

Departamento de Física, Universidad Técnica, Federico Santa María, and Centro-Científico-Tecnológico de Valparaíso, Casilla 110-V, Valparaíso, Chile

(Received 22 March 2011; published 19 September 2011)

Matrix element $U_{\tau N}$ of sterile neutrino N mixing with ν_τ is the least constrained in the literature amo ng the three $U_{\alpha N}$ ($\alpha = e, \mu, \tau$) mixing parameters characterizing the sterile neutrino phenomenology. We study the contribution of massive dominantly sterile neutrinos to purely leptonic τ decays and semi-leptonic decays of τ and K, D mesons. We consider some decays allowed in the standard model as well as lepton flavor and lepton number violating decays forbidden in the standard model. From the existing experimental data on the branching ratios of these processes we derived new limits on $U_{\tau N}$ more stringent than the ones existing in the literature. These limits are extracted in a model independent way without any *ad hoc* assumptions on the relative size of the three different sterile neutrino mixing parameters.

DOI: 10.1103/PhysRevD.84.053008 PACS numbers: 13.35.Hb, 13.15.+g, 13.20.−v, 13.35.Dx

I. INTRODUCTION

Lepton flavors are conserved in the standard model (SM) due to the presence of an accidental lepton flavor symmetry, which, however, is broken by nonzero neutrino masses. Neutrino oscillation experiments have proven that neutrinos are massive, although very light, particles mixing with each other. Moreover, neutrino oscillations are the first and so far the only observed phenomenon of lepton flavor violation (LFV). In the sector of charged leptons LVF is strongly suppressed by the smallness of neutrino square mass differences $(m^2_{\nu_i} - m^2_{\nu_j})/q_0^2$ compared to the characteristic momentum scale, q_0, of an LFV process which is typically of the order of the charged lepton mass $q_0 \sim m_l$. If neutrinos are Majorana particles there can also occur lepton number violating (LNV) processes. They are also suppressed by the smallness of the absolute value of m_ν. However, the situation may dramatically change if there exist either heavy neutrinos N_i, known as sterile, mixed with the active flavors $\nu_{e,\mu,\tau}$ or if there are some new LFV and LNV interactions beyond the SM.

Here we study the former possibility and consider an extension of the SM with right-handed neutrinos. In the case of n species of the SM singlet right-handed neutrinos $\nu'_{Rj} = (\nu'_{R1}, \ldots \nu'_{Rn})$, besides the three left-handed weak doublet neutrinos $\nu'_{Li} = (\nu'_{Le}, \nu'_{L\mu}, \nu'_{L\tau})$ the neutrino mass term can be written as [1,2]

$$-\frac{1}{2}\overline{\nu'}\mathcal{M}^{(\nu)}\nu'^c + \text{H.c.}$$
$$= -\frac{1}{2}(\overline{\nu'_L}, \overline{\nu'^c_R})\begin{pmatrix} \mathcal{M}_L & \mathcal{M}_D \\ \mathcal{M}_D^T & \mathcal{M}_R \end{pmatrix}\begin{pmatrix} \nu'^c_L \\ \nu'_R \end{pmatrix} + \text{H.c.} \quad (1)$$

$$= -\frac{1}{2}\left(\sum_{i=1}^{3} m_{\nu_i}\overline{\nu^c_i}\nu_i + \sum_{j=1}^{n} m_{\nu_j}\overline{\nu^c_j}\nu_j\right) + \text{H.c.} \quad (2)$$

Here $\mathcal{M}_L$, $\mathcal{M}_R$ are 3×3 and $n\times n$ symmetric Majorana mass matrices, and M_D is a $3\times n$ Dirac type matrix. Rotating the neutrino mass matrix to the diagonal form by a unitary transformation

$$U^T\mathcal{M}^{(\nu)}U = \text{Diag}\{m_{\nu_1}, \ldots, m_{\nu_{3+n}}\}, \quad (3)$$

one ends up with $3 + n$ Majorana neutrinos with masses $m_{\nu_1}, \ldots, m_{\nu_{3+n}}$. The matrix $U_{\alpha k}$ is a neutrino mixing matrix. In special cases among neutrino mass eigenstates there may appear pairs with masses degenerate in absolute values. Each of these pairs can be collected into a Dirac neutrino field. This situation corresponds to conservation of certain lepton numbers assigned to these Dirac fields. Generically in this setup neutrino mass eigenstates can be of any mass. For consistency with neutrino phenomenology (for a recent review, cf. [3]) among them there must be the three very light neutrinos with different masses and dominated by the active flavors ν_α ($\alpha = e, \mu, \tau$). The remaining states may also have a certain admixture of the active flavors and, therefore, participate in charged and neutral current interactions of the SM contributing to LNV and LFV processes. Explanation of the presence in the neutrino spectrum of the three very light neutrinos requires additional physically motivated assumptions on the structure of the mass matrix in (1). The celebrated "seesaw" mechanism [4], presently called type-I seesaw, is implemented in this framework assuming that $\mathcal{M}_R \gg \mathcal{M}_D$. Then, there naturally appear light neutrinos with masses of the order of $\sim\mathcal{M}_D^2/\mathcal{M}_R$ dominated by ν_α. Also, there must be present heavy Majorana neutrinos with masses at the scale of $\sim\mathcal{M}_R$. Their mixing with active neutrino flavors is suppressed by a factor $\sim\mathcal{M}_D/\mathcal{M}_R$ which should be very small. In particular scenarios this generic limitation of the seesaw mechanism can be relaxed [5]. Then the heavy neutrinos could be, in principle, observable at LHC, if their masses are within the kinematical reach the corresponding experiments. Very heavy or moderately heavy Majorana entry $\mathcal{M}_R$ of the neutrino mass matrix naturally appears in various extensions of the SM. The well known examples are given by the $SO(10)$-based

supersymmetric [6] and ordinary [7] grand unification models as well as models with spontaneous breaking of lepton numbers [8]. The supersymmetric versions of see-saw are also widely discussed in the literature (cf. [9] and references therein).

In the present paper we study the above mentioned generic case of the neutrino mass matrix in (1) without implying a specific scenario of neutrino mass generation. We assume there is at least one moderately heavy neutrino N in the MeV–GeV domain or even lighter. The presence or absence of these neutrino states, conventionally called sterile neutrinos, is a question for experimental searches. If they exist, they may contribute to some LNV and LFV processes as intermediate nearly on-mass-shell states. This would lead to resonant enhancement of their contributions to these processes. As a result, it may become possible to either observe the LNV, LFV processes or set stringent limits on sterile neutrino mass m_N and mixing $U_{\alpha N}$ with active neutrino flavors ν_α ($\alpha = e, \mu, \tau$) from nonobservation of the corresponding processes.

On the other hand, the sterile neutrinos in this mass range are motivated by various phenomenological models [10], in particular, by the recently proposed electroweak scale see-saw models [11,12]. They may also play an important astrophysical and cosmological role. The sterile neutrinos in this mass range may have an impact on big bang nucleosynthesis, large scale structure formation [13], supernovae explosions [14]. Moreover, the keV–GeV sterile neutrinos are good dark matter candidates [15–17] and offer a plausible explanation of baryogenesis [18]. Dark matter sterile neutrinos, having a small admixture of active flavors, may suffer radiative decays and contribute to the diffuse extragalactic radiation and x-rays from galactic clusters [19]. This is, of course, an incomplete list of cosmological and astrophysical implications of sterile neutrinos. More details on this subject can be found in Refs. [20–22].

The phenomenology of sterile neutrinos in the processes, which can be searched for in laboratory experiments have been studied in the literature in different contexts and from complementary points of view (for earlier studies see [23]). Their resonant contributions to τ and meson decays have been studied in Refs. [2,24–28]. Another potential process to look for sterile Majorana neutrinos is like-sign dilepton production in hadron collisions [29–32]. Possible implications of sterile neutrinos have been also studied in LFV muonium decay and high-energy muon-electron scattering [33]. Constraints on the sterile neutrino parameters have been derived from the accelerator and Super-Kamiokande measurements [34]. An interesting explanation of anomalous excess of events observed in the LSND [35] and MiniBooNE [36] neutrino experiments has been recently proposed [37] in terms of sterile neutrinos with masses from 40 to 80 MeV. An explanation comes out of their possible production in neutral current interactions of ν_μ and subsequent radiative decay to light neutrinos.

Here we study a scenario with only one sterile neutrino state N. Phenomenology of a single sterile neutrino N is specified by its mass m_N and three mixing matrix elements U_{eN}, $U_{\mu N}$, $U_{\tau N}$. In the present paper we focus on the derivation of limits on the matrix element $U_{\tau N}$, which is currently least constrained in the literature. Towards this end we use the results of experimental measurements of branching ratios of purely leptonic τ decays and semileptonic decays of τ and K, D mesons [38]. One of the key points of our derivation is its model independent character, in the sense that we do not apply any additional assumptions on the relative size of the three mixing parameters $U_{\alpha N}$. Such *ad hoc* assumptions are typical in the literature and stem from the fact that all these three parameters enter in the decay rate formulas of any decay, potentially receiving contribution from N as an intermediate state. Therefore, in order to extract individual limits on each mixing parameter one may need additional information on them. We will show that in purely leptonic τ decays it is unnecessary and in the other cases this sort of information can be procured by a joint analysis of certain sets of leptonic and semileptonic decays of τ and K, D.

The paper is organized as follows. In Sec. II we present decay rate formulas for τ and pseudoscalar meson LFV and LNV decays in the resonant domains of sterile neutrino mass m_N. In Sec. III we derive upper limits on $|U_{\tau N}|$ from the existing experimental data on purely leptonic 5-body τ decays, semileptonic τ and K, D decays, considering sterile neutrino contribution as an intermediate state and in some cases as one of the final state particles. Section IV contains the summary and discussion of our main results.

II. DECAY RATES

Neutrino interactions are represented by the SM charged and neutral current Lagrangian terms. In the mass eigenstate basis they read

$$\mathcal{L} = \frac{g_2}{\sqrt{2}} \sum_i U_{li} \bar{l} \gamma^\mu P_L \nu_i W_\mu^- + \frac{g_2}{2\cos\theta_W} \sum_{\alpha,i,j} U_{\alpha j} U_{\alpha i}^* \bar{\nu}_i \gamma^\mu P_L \nu_j Z_\mu, \tag{4}$$

where $l = e, \mu, \tau$ and $i = 1, \ldots, n+3$. We consider the case with a single sterile neutrino N and, therefore, we choose $n = 1$ and identify $N = \nu_4$.

In what follows we study the sterile neutrino contribution to the following decays

$$\tau^- \to l^- e^- e^+ \nu\nu, \qquad \tau^- \to l^\mp \pi^\pm \pi^-, \qquad M^+ \to l_1^+ l_2^\pm \pi^\mp, \tag{5}$$

$$\tau^- \to \pi^- N, \qquad \tau^- \to l^- \bar{\nu}_l N, \tag{6}$$

where $M = K, D, B$ and $l, l_i = e, \mu$. In the first decay of Eq. (5) both νs denote the standard neutrino or antineutrino dominated by any of the neutrino flavors ν_e, ν_μ, ν_τ. These

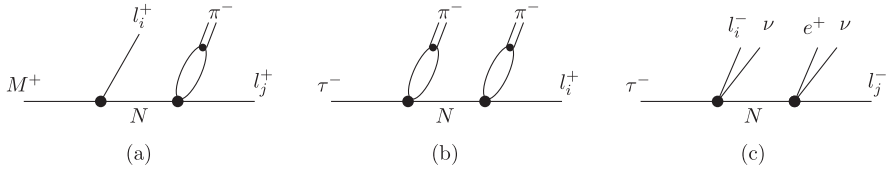

FIG. 1. Structure of the lowest order contribution of sterile neutrino N to the semileptonic and leptonic meson and τ decays. Here l_i, $l_j = e$, μ.

reactions include lepton number and flavor conserving as well as LFV and LNV decays. In the first case they receive the SM contributions, which alone give good agreement with the experimental data.

The LFV and LNV decays (5) are only possible beyond the SM. In the present framework they proceed according to the diagrams shown in Fig. 1 with the sterile neutrino N as a virtual particle. Considering LNV decays we assume that the sterile neutrino is a Majorana particle $N = N^c$. When the intermediate sterile neutrino N in these diagrams is off shell their contribution to the processes (5) is negligibly small [2], being far away from experimental reach. On the other hand, there exist specific domains of sterile neutrino mass m_N where N comes, for kinematical reasons, close to its mass-shell leading to resonant enhancement [2,24,25] of the diagrams in Fig. 1. These domains of m_N will be specified below.

The decay rate formulas for the reactions in Eq. (5) can be directly calculated from the diagrams in Fig. 1 and the Lagrangian (4) for arbitrary mass m_N of the sterile neutrino. We focus on the regions of m_N where the sterile neutrino contribution is resonantly enhanced [2,24,25]. In these mass domains the intermediate sterile neutrino in Fig. 1 can be treated as nearly an on-mass-shell state. This is to say, the sterile neutrino N is produced in the left vertices of the diagrams in Fig. 1, propagates as a free unstable particle and then finally decays in the right vertices. Thus the decay rate formulas for the reactions τ, $M \to X_1 X_2 l$ can be represented in the form of products of the two factors: τ or meson decay rate to the sterile neutrino $\Gamma(\tau, M \to N X_1)$ and a branching ratio of the sterile neutrino decay $\mathrm{Br}(N \to l X_2)$, where X_i, l represent final state particles of (5). This representation is approximate and valid in the "narrow width approximation" $\Gamma_N \ll m_N$, where Γ_N is the total decay width of sterile neutrino [2]. The interference term between a diagram representing some process and a similar diagram with interchanged particles in the final state, like $l_i \leftrightarrow l_j$ in Fig. 1(a), vanishes in this approximation (for details see [2]). As seen from Fig. 2, the condition $\Gamma_N \ll m_N$ is satisfied in the region of m_N studied in our analysis where $\Gamma_N < 10^{-10}$ MeV. Below we list the decay rate formulas in this approximation for the reactions in Eq. (5) specifying the corresponding resonant regions of m_N where they are applicable. These formulas are readily derived from the diagrams in Fig. 1, considering the two vertices as the two

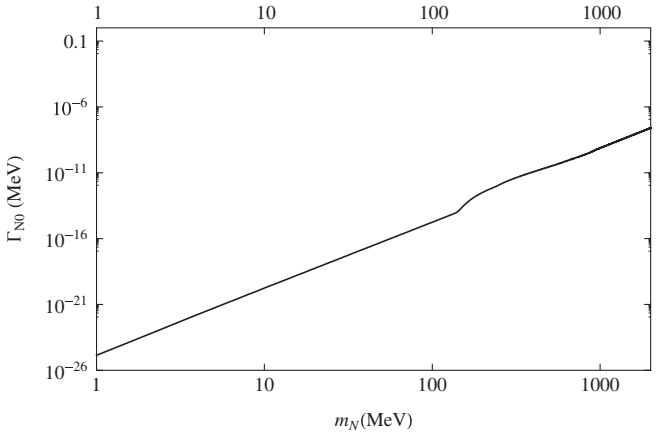

FIG. 2. Sterile neutrino decay rate Γ_N for the particular case of $U_{eN} = U_{\mu N} = U_{\tau N} = 1$ denoted by Γ_{N0}. For definitions and discussion, see the Appendix.

independent processes of sterile neutrino production and its subsequent decay.

For semileptonic decays of mesons M and τ lepton, the decay rate formulas are

$$\Gamma(M^+ \to \pi^- e^+ e^+) \approx \Gamma(M^+ \to l^+ N) \frac{\Gamma(N^c \to e^+ \pi^-)}{\Gamma_N}, \quad (7)$$

$$\Gamma(M^+ \to \pi^- \mu^+ e^+) \approx \Gamma(M^+ \to e^+ N) \frac{\Gamma(N^c \to \mu^+ \pi^-)}{\Gamma_N} + \Gamma(M^+ \to \mu^+ N) \frac{\Gamma(N^c \to e^+ \pi^-)}{\Gamma_N}, \quad (8)$$

$$\Gamma(M^+ \to \pi^+ \mu^- e^+) \approx \Gamma(M^+ \to e^+ N) \frac{\Gamma(N \to \mu^- \pi^+)}{\Gamma_N}, \quad (9)$$

valid in $m_e + m_\pi < m_N < m_M - m_e$,

$$\Gamma(\tau^- \to \pi^- \pi^\pm l^\mp) \approx \Gamma(\tau^- \to \pi^- N) \times \left\{ \frac{\Gamma(N \to l^- \pi^+)}{\Gamma_N}, \frac{\Gamma(N^c \to l^+ \pi^-)}{\Gamma_N} \right\}, \quad (10)$$

valid in $m_l + m_\pi < m_N < m_\tau - m_\pi$. Studying in Sec. III A purely leptonic τ decays shown in Eq. (5), we will need the decay rates summed over all the standard light neutrinos and antineutrinos in the final state. The corresponding formulas take the form

$$\Gamma(\tau^- \to e^- e^+ e^- \nu\nu) \approx (1+\delta_N)\sum_l \left[\Gamma(\tau^- \to e^- \bar{\nu}_e N)\frac{\Gamma(N \to e^+ e^- \nu_l)}{\Gamma_N} + \Gamma(\tau^- \to e^- \nu_\tau N^c)\frac{\Gamma(N^c \to e^+ e^- \bar{\nu}_l)}{\Gamma_N}\right], \quad (11)$$

$$\begin{aligned}\Gamma(\tau^- \to e^- e^+ \mu^- \nu\nu) \approx{}& \Gamma(\tau^- \to e^- \bar{\nu}_e N)\frac{\Gamma(N \to e^+ \mu^- \nu_e)}{\Gamma_N} + \delta_N \cdot \Gamma(\tau^- \to e^- \bar{\nu}_e N)\frac{\Gamma(N^c \to e^+ \mu^- \bar{\nu}_\mu)}{\Gamma_N} \\ &+ \delta_N \cdot \Gamma(\tau^- \to e^- \nu_\tau N^c)\frac{\Gamma(N \to e^+ \mu^- \nu_e)}{\Gamma_N} + \Gamma(\tau^- \to e^- \nu_\tau N^c)\frac{\Gamma(N^c \to e^+ \mu^- \bar{\nu}_\mu)}{\Gamma_N} \\ &+ (1+\delta_N)\sum_l \left[\Gamma(\tau^- \to \mu^- \bar{\nu}_\mu N)\frac{\Gamma(N \to e^+ e^- \nu_l)}{\Gamma_N} + \Gamma(\tau^- \to \mu^- \nu_\tau N^c)\frac{\Gamma(N^c \to e^+ e^- \bar{\nu}_l)}{\Gamma_N}\right], \quad (12)\end{aligned}$$

valid in $2m_e < m_N < m_\tau - m_e$. Here $\delta_M = 0, 1$ for the Dirac and Majorana case of sterile neutrino N, respectively. Summation in (11) and (12) runs over $l = e, \mu, \tau$. The partial decay rates $\Gamma(\tau, M \to XN)$ and $\Gamma(N \to Yl)$ and the total decay rate of sterile neutrino Γ_N involved in Eqs. (7)–(12) are specified in the Appendix. Implicitly all the partial decay rates include the corresponding threshold step functions. For further convenience we rewrite Eq. (11) and (12) in the form

$$\begin{aligned}\Gamma(\tau^- \to e^- e^+ e^- \nu\nu) \approx{}& (1+\delta_N)\frac{\Gamma_\tau^{(e\nu N)}\Gamma_N^{(ee\nu_\tau)}}{\Gamma_N}(|U_{\tau N}|^4 + |U_{\mu N}|^2|U_{\tau N}|^2 + (\beta+1)|U_{eN}|^2|U_{\tau N}|^2 \\ &+ |U_{eN}|^2|U_{\mu N}|^2 + \beta|U_{eN}|^4), \quad (13)\end{aligned}$$

$$\begin{aligned}\Gamma(\tau^- \to e^- e^+ \mu^- \nu\nu) \approx{}& \frac{\Gamma_\tau^{(e\nu N)}\Gamma_N^{(e\mu\nu)} + \Gamma_\tau^{(\mu\nu N)}\Gamma_N^{(ee\nu_\tau)}}{\Gamma_N}((1+\delta_N)\alpha_2|U_{\tau N}|^4 + (\alpha_1 + 2(1+\delta_N)\alpha_2)|U_{\mu N}|^2|U_{\tau N}|^2 \\ &+ (\delta_N\alpha_1 + (1+\delta_N)\beta\alpha_2)|U_{eN}|^2|U_{\tau N}|^2 + (\delta_N\alpha_1 + (1+\delta_N)\beta\alpha_2)|U_{eN}|^2|U_{\mu N}|^2 \\ &+ \alpha_1|U_{eN}|^4 + (1+\delta_N)\alpha_2|U_{\mu N}|^4), \quad (14)\end{aligned}$$

where

$$\beta = \Gamma_N^{(ee\nu_e)}/\Gamma_N^{(ee\nu_\tau)} \approx 4.65, \quad (15)$$

$$\begin{aligned}\alpha_1 &= \frac{\Gamma_\tau^{(e\nu N)}\Gamma_N^{(e\mu\nu)}}{\Gamma_\tau^{(e\nu N)}\Gamma_N^{(e\mu\nu)} + \Gamma_\tau^{(\mu\nu N)}\Gamma_N^{(ee\nu_\tau)}}, \\ \alpha_2 &= \frac{\Gamma_\tau^{(\mu\nu N)}\Gamma_N^{(ee\nu_\tau)}}{\Gamma_\tau^{(e\nu N)}\Gamma_N^{(e\mu\nu)} + \Gamma_\tau^{(\mu\nu N)}\Gamma_N^{(ee\nu_\tau)}}.\end{aligned} \quad (16)$$

In Eqs. (13)–(16) we used notations $\Gamma_N^{(ll\nu)}$, $\Gamma_\tau^{(l\nu N)}$ introduced in Eqs. (A1)–(A11).

As we already mentioned, in the resonant regions of the sterile neutrino mass m_N, specified in Eqs. (7)–(12), the intermediate sterile neutrino N, produced in τ and meson M decays (see Fig. 1), propagates as a real particle and decays at a certain distance from the production point. If this distance is larger than the size of the detector, the sterile neutrino escapes from it before decaying and the signature of $\tau \to l\pi\pi$, $\tau \to eel\nu\nu$ or $M \to \pi ll$ cannot be recognized. In this case in order to calculate the rate of τ or meson decay within a detector one should multiply the theoretical expressions Γ in (7)–(12) by the probability P_N of sterile neutrino decay within a detector of the size L_D. Within reasonable approximations it takes the form [28]

$$P_N \approx 1 - \exp(-L_D\Gamma_N), \quad (17)$$

where Γ_N is the total decay rate of the sterile neutrino calculated in (A17).

Then, the rates Γ^D of τ and meson decays within the detector volume should be estimated according to

$$\Gamma^D = \Gamma \times P_N, \quad (18)$$

where Γ are decay rates given by Eqs. (7)–(12). In our numerical analysis we take for concreteness $L_D = 10$ m which is typical for this kind of experiments. In Fig. 3 we plotted P_N vs the sterile neutrino mass m_N for several values of mixing matrix elements $|U_{lN}|^2$. For illustration of typical tendencies we assumed in this plot $|U_{eN}|^2 = |U_{\mu N}|^2 = |U_{\tau N}|^2$. We do not use this assumption in our analysis. As seen, P_N becomes small for $m_N < 100$ MeV even for rather large values of $|U|^2_{lN}$. Thus, in this region of m_N the effect of the finite size of the detector, described by P_N, significantly affects the decay rates of the studied processes and should be taken into account.

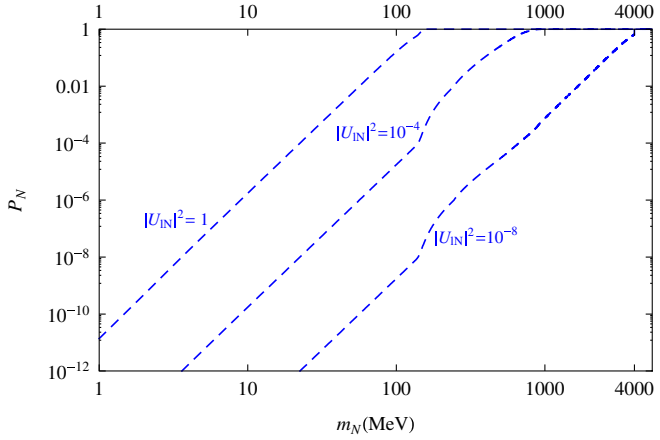

FIG. 3 (color online). The probability P_N of sterile neutrino decay within a detector of the size of $L_D = 10$ m versus sterile neutrino mass m_N for several values of mixing matrix elements $|U_{lN}|^2$, assuming $|U_{eN}|^2 = |U_{\mu N}|^2 = |U_{\tau N}|^2$.

III. LIMITS ON STERILE NEUTRINO MIXING $U_{\tau N}$

In the literature there are various limits on the mixing parameters $U_{\alpha N}$ (with $\alpha = e, \mu, \tau$) extracted from direct and indirect experimental searches [38] for sterile neutrino N, in a wide region of its mass m_N. A recent summary of these limits can be found in Ref. [28]. In the present paper we focus on the least constrained mixing parameter $U_{\tau N}$. The corresponding experimental bounds for $|U_{\tau N}|^2$ are displayed in Fig. 4. The 90% C.L. exclusion curves from the CHARM [39] and the NOMAD [40] experiments are based on the searches for a heavy neutral lepton N from τ and D decays. The DELPHI collaboration [41] derived bounds on $|U_{eN}|^2$, $|U_{\mu N}|^2$, $|U_{\tau N}|^2$ at 95% C.L. from the searches for decays of a heavy neutral lepton N produced in $Z^0 \to N\bar{\nu}$. The DELPHI exclusion curve for $|U_{\tau N}|^2$ shown in Fig. 4 properly takes into account τ-production kinematical suppression for the low m_N. We borrowed this curve from Ref. [28]. This suppression was also discussed in the original paper of the DELPHI collaboration [41], but not explicitly given in a graphical form for $|U_{\tau N}|^2$.

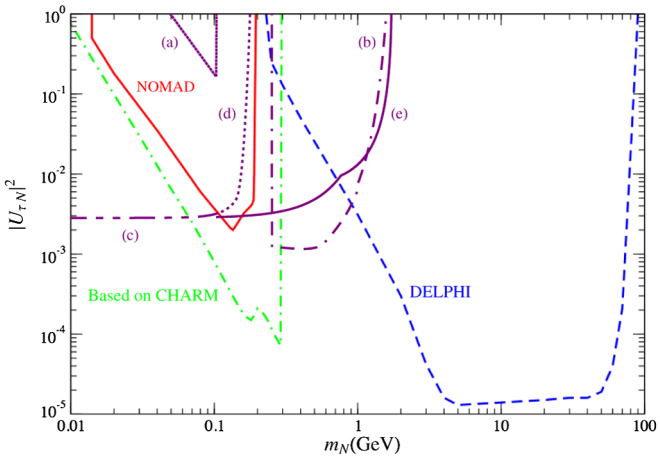

FIG. 4 (color online). Exclusion curves for $|U_{\tau N}|^2$ from the present analysis, denoted by (a)–(e), and the exclusion curves existing in the literature derived from CHARM [39], NOMAD [40] and DELPHI [41] searches for sterile neutrino decays. The latter curves are taken from Ref. [28].

In Fig. 4 we also show our exclusion curves derived in the present section. For derivation of these curves we analyze the sterile neutrino contribution to the decays listed in (5) and (6). As seen from Eqs. (7)–(12) the decay rates of the processes (5) depend on all three $U_{\alpha N}$ (with $\alpha = e, \mu, \tau$) mixing matrix elements. In the literature it is common practice to adopt some *ad hoc* assumptions on their relative size in order to extract limits on them from the experimental bounds on the corresponding decay rates. In particular, the limits from CHARM [39] and NOMAD [40] plotted in Fig. 4 assume $|U_{\tau N}| \gg |U_{eN}|, |U_{\mu N}|$. These assumptions may reduce reliability of the obtained limits. Below we derive analytic expressions for limits on $|U_{\tau N}|^2$ in different mass ranges of m_N without any kind of such assumptions.

A. Purely leptonic decays

First we exploit for extraction of $|U_{\tau N}|$ the following experimental results for the branching ratios of purely leptonic τ decays [38]

$$\mathrm{Br}(\tau^- \to e^- e^+ e^- \bar{\nu}_e \nu_\tau) = (2.8 \pm 1.5) \times 10^{-5}, \quad (19)$$

$$\mathrm{Br}(\tau^- \to e^- e^+ \mu^- \bar{\nu}_\mu \nu_\tau) < 3.6 \times 10^{-5}. \quad (20)$$

The first decay has been observed experimentally and its experimentally measured branching ratio agrees with the SM prediction within the standard deviation $\Delta^{\mathrm{exp}}(\tau^- \to e^- e^+ e^- \nu\nu) = 1.5 \times 10^{-5}$. Neutrino assignment in the final states of the decays (19) and (20) corresponds to what is suggested by the SM. However, in the experiments, measuring these decays, the final state neutrinos cannot be actually identified. Therefore, considering beyond the SM mechanisms with LFV one should take into account the possibility that all the light neutrinos ν_e, ν_μ and ν_τ may contribute to the final state of the decays (19) and (20). Equations (13) and (14) were derived for this very case. They describe the sterile neutrino resonant contribution (Fig. 1(a)) to the decays (19) and (20) and will be used in the analysis of this subsection.

We also assume that the sterile neutrino contribution to the process (19), if it exists, should be less than Δ^{exp}. For the decay (20), not yet observed experimentally, there exists only the above indicated upper bound and the sterile neutrino contribution has to obey this bound.

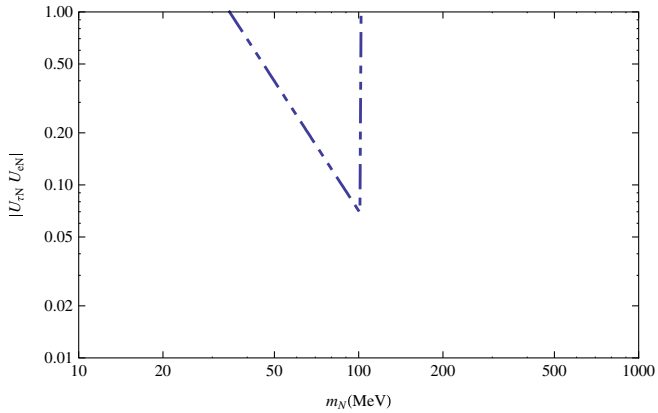

FIG. 5 (color online). Exclusion curves for $|U_{\tau N}U_{eN}|$ from the present analysis.

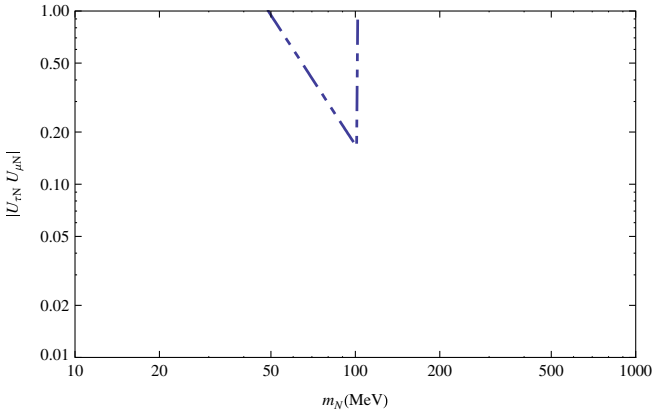

FIG. 6 (color online). Exclusion curves for $|U_{\tau N}U_{\mu N}|$ from the present analysis.

Taking into account the finite detector size effect according to Eq. (18) we write for the decay rate Γ^D within the detector volume

$$\Gamma^D(\tau^- \to e^- e^+ l^- \nu\nu) \approx \Gamma(\tau^- \to e^- e^+ l^- \nu\nu) \times P_N, \tag{21}$$

with $\Gamma(\tau^- \to e^- e^+ l^- \nu\nu)$ given by (11) and (12). As we discussed in the previous section, the probability P_N of sterile neutrino decay within the detector becomes rather small for $m_N < 100$ MeV. Therefore, in this mass range we may approximate the expression in (17) by $P_N \approx L_D\Gamma_N$. This is a reasonable approximation for this part of our analysis since the limits, which will be obtained here, correspond to the exclusion curve (a) in Fig. 4 and curves in Figs. 5 and 6 located in the region $m_N \leq 100$ MeV, where $L_D\Gamma_N \sim 0.01$.

In this approximation we find from (13) and (21)

$$\begin{aligned}\Gamma^D(\tau^- \to e^- e^+ e^- \nu\nu) &\approx (1+\delta_N)\Gamma_\tau^{(e\nu N)}\Gamma_N^{(ee\nu_\tau)} L_D(|U_{\tau N}|^4 + |U_{\mu N}|^2|U_{\tau N}|^2 \\ &\quad + (\beta+1)|U_{eN}|^2|U_{\tau N}|^2 + |U_{eN}|^2|U_{\mu N}|^2 + \beta|U_{eN}|^4).\end{aligned} \tag{22}$$

According to our assumption, discussed after Eqs. (19) and (20), we require

$$\begin{aligned}\tau_\tau\Gamma(\tau^- \to e^- e^+ e^- \nu\nu) &\leq \Delta^{\exp}(\tau^- \to e^- e^+ e^- \nu\nu) \\ &\approx 1.5 \times 10^{-5},\end{aligned} \tag{23}$$

where $\tau_\tau = (290.6 \pm 1.0) \times 10^{-15}$ s is the τ-lepton mean life [38]. Then we obtain the following upper limits

$$|U_{\tau N}|^2 \leq \sqrt{\frac{\Delta^{\exp}(\tau^- \to e^- e^+ e^- \nu\nu)}{\Gamma_\tau^{(e\nu N)}\Gamma_N^{(ee\nu_\tau)}(1+\delta_N)L_D\tau_\tau}}, \tag{24}$$

$$\begin{aligned}|U_{\tau N}U_{\mu N}| &\leq \sqrt{\frac{\Delta^{\exp}(\tau^- \to e^- e^+ e^- \nu\nu)}{\Gamma_\tau^{(e\nu N)}\Gamma_N^{(ee\nu_\tau)}(1+\delta_N)L_D\tau_\tau}}, \\ |U_{\tau N}U_{eN}| &\leq \sqrt{\frac{\Delta^{\exp}(\tau^- \to e^- e^+ e^- \nu\nu)}{(\beta+1)\Gamma_\tau^{(e\nu N)}\Gamma_N^{(ee\nu_\tau)}(1+\delta_N)L_D\tau_\tau}}.\end{aligned} \tag{25}$$

Similarly, we derive limits based on the experimental bound (20). Using Eq. (14), we find

$$|U_{\tau N}|^2 \leq \sqrt{\frac{\mathrm{Br}^{\exp}(\tau^- \to \mu^- e^+ e^- \nu\nu)}{(\Gamma_\tau^{(e\nu N)}\Gamma_N^{(e\mu\nu)} + \Gamma_\tau^{(\mu\nu N)}\Gamma_N^{(ee\nu_\tau)})(1+\delta_N)\alpha_2 L_D\tau_\tau}}, \tag{26}$$

$$|U_{\tau N}U_{\mu N}| \leq \sqrt{\frac{\mathrm{Br}^{\exp}(\tau^- \to \mu^- e^+ e^- \nu\nu)}{(\Gamma_\tau^{(e\nu N)}\Gamma_N^{(e\mu\nu)} + \Gamma_\tau^{(\mu\nu N)}\Gamma_N^{(ee\nu_\tau)})(\alpha_1 + 2(1+\delta_N)\alpha_2)L_D\tau_\tau}}, \tag{27}$$

$$|U_{\tau N}U_{eN}| \leq \sqrt{\frac{\mathrm{Br}^{\exp}(\tau^- \to \mu^- e^+ e^- \nu\nu)}{(\Gamma_\tau^{(e\nu N)}\Gamma_N^{(e\mu\nu)} + \Gamma_\tau^{(\mu\nu N)}\Gamma_N^{(ee\nu_\tau)})(\delta_N\alpha_1 + (1+\delta_N)\beta\alpha_2)L_D\tau_\tau}}. \tag{28}$$

Here, $\mathrm{Br}^{\mathrm{exp}}$ denotes the left-hand side of the experimental bound in (20). The limits (24)–(28) are plotted in Figs. 4–6 for the case of the sterile Majorana neutrinos. Drawing the exclusion curves, we selected the most stringent limit among (24)–(28) for each mass value m_N within the studied mass range. As seen, the present experimental data (19) and (20) on purely leptonic τ decays set rather weak constraints on $|U_{\tau N}|$ and on $|U_{\tau N}U_{eN}|$, $|U_{\tau N}U_{\mu N}|$ in the mass region 1 MeV $\leq m_N \leq$ 100 MeV. Our limits on $|U_{\tau N}|$, corresponding to curve (a) in Fig. 4, are significantly weaker than the limitations from other searches shown in Fig. 4. However, our limits for $|U_{\tau N}U_{eN}|$ and $|U_{\tau N}U_{\mu N}|$ in Figs. 5 and 6 to our best knowledge are new in this mass region.

B. Leptonic and semileptonic decays

Now we combine the purely leptonic τ decays considered in the previous subsection with the semileptonic decays of τ and K, D mesons using the experimental data (19) and (20) and the experimental limits on the following branching ratios [38]:

$$\begin{aligned} &\mathrm{Br}(\tau^- \to \pi^-\pi^+e^-) \leq 1.2\times 10^{-7},\\ &\mathrm{Br}(\tau^- \to \pi^-\pi^+\mu^+) \leq 7\times 10^{-8}, \end{aligned} \tag{29}$$

$$\begin{aligned} &\mathrm{Br}(K^+ \to \pi^-e^+e^+) \leq 6.4\times 10^{-10},\\ &\mathrm{Br}(K^+ \to \pi^+\mu^-e^+) \leq 1.3\times 10^{-11}, \end{aligned} \tag{30}$$

$$\begin{aligned} &\mathrm{Br}(D^+ \to \pi^-e^+e^+) \leq 3.6\times 10^{-6},\\ &\mathrm{Br}(D^+ \to \pi^+\mu^-e^+) \leq 3.4\times 10^{-5}. \end{aligned} \tag{31}$$

Assuming that in all these decays sterile neutrino N contributes resonantly we should limit ourselves to the mass domain:

$$m_\pi + m_\mu \approx 245\ \mathrm{MeV} \leq m_N \leq m_\tau - m_\pi \approx 1637\ \mathrm{MeV}. \tag{32}$$

Within this mass domain the experimental bounds (30) contribute to our analysis only up to $m_N \leq m_K - m_e \approx$ 493.2 MeV corresponding to the mass range of the resonant contribution of the sterile neutrino to these decays of the K meson. In the above list (29)–(31) one could also include the existing experimental bounds on the other LNV and LFV decays of τ and D_s, B mesons. However, they have negligible impact on our results presented below.

In this part of our analysis we put $P_N = 1$ for the probability (see Eq. (17)) of decay of the nearly on-mass-shell sterile neutrino, resonantly contributing to the analyzed processes. Thus we assume that these processes occur completely within a detector volume. This is a good approximation for the case of the limits on $U_{\tau N}$, which will be derived here and displayed in Fig. 4 as curve (b). To see this one can check the plot for P_N shown in Fig. 3.

In the mass domain (32) we can use Eqs. (7)–(14) for the corresponding decay rates. Below we combine these formulas in a system of equations. Solving them with respect to $|U_{\tau N}|$ and applying the experimental bounds (19), (20), and (29)–(31) we find upper limits on this mixing parameter. For our purpose it is sufficient to use either of the two experimental bounds (19) and (20). We select (19) which leads to a bit more stringent limits on $|U_{\tau N}|$.

Let us introduce the following notations

$$\begin{aligned} F_{ee}(\tau) &= \frac{\Delta^{\mathrm{exp}}(\tau^- \to e^-e^+e^-\nu\nu)}{(1+\delta_N)\Gamma_\tau^{(l\nu N)}\Gamma_N^{(ee\nu_\tau)}\tau_\tau},\\ F_{\pi l}(\tau) &= \frac{\mathrm{Br}^{\mathrm{exp}}(\tau^- \to \pi^-\pi^{\pm}l^{\mp})}{\Gamma_\tau^{(\pi N)}\Gamma_N^{(l\pi)}\tau_\tau},\\ F_{ee}(M) &= \frac{\mathrm{Br}^{\mathrm{exp}}(M^+ \to \pi^-e^+e^+)}{\Gamma_M^{(eN)}\Gamma_N^{(e\pi)}\tau_M},\\ F_{e\mu}(M) &= \frac{\mathrm{Br}^{\mathrm{exp}}(M^+ \to \pi^-\mu^+e^+)}{(\Gamma_M^{(eN)}\Gamma_N^{(\mu\pi)}+\Gamma_M^{(\mu N)}\Gamma_N^{(e\pi)})\tau_M}, \end{aligned} \tag{33}$$

where τ_τ, τ_M are mean lives of τ and $M = K^+, D^+$; the right-hand sides of the experimental bounds in (29)–(31) are denoted by $\mathrm{Br}^{\mathrm{exp}}$; the quantity Δ^{exp} was introduced after Eqs. (19) and (20).

Now we can rewrite the experimental limits on (19) and (29)–(31) in the form

$$\frac{|U_{\tau N}|^4 + |U_{\mu N}|^2|U_{\tau N}|^2 + (\beta+1)|U_{eN}|^2|U_{\tau N}|^2 + |U_{eN}|^2|U_{\mu N}|^2 + \beta|U_{eN}|^4)}{a_e|U_{eN}|^2 + a_\mu|U_{\mu N}|^2 + a_\tau|U_{\tau N}|^2} \leq F_{ee}(\tau), \tag{34}$$

$$\frac{|U_{\tau N}|^2|U_{lN}|^2}{a_e|U_{eN}|^2 + a_\mu|U_{\mu N}|^2 + a_\tau|U_{\tau N}|^2} \leq F_{\pi l}(\tau), \tag{35}$$

$$\frac{|U_{eN}|^2|U_{lN}|^2}{a_e|U_{eN}|^2 + a_\mu|U_{\mu N}|^2 + a_\tau|U_{\tau N}|^2} \leq F_{el}(M). \tag{36}$$

Here $l = e$, μ and the parameters $a_{e,\mu,\tau}$ are defined in (A17) and (A18). Solving (34)–(36) we find

$$|U_{\tau N}|^2 \leq c_1F_{ee}(\tau) + c_2F_{\pi e}(\tau) + c_3F_{\pi\mu}(\tau) + c_4F_{ee}(M) + c_5F_{e\mu}(M), \tag{37}$$

where

$$c_1 = a_\tau, \qquad c_2 = a_e - 2a_\tau, \qquad c_3 = a_\mu - a_\tau,$$
$$c_4 = (\beta - 1)a_e - \beta a_\tau, \qquad c_5 = (\beta - 1)a_\mu - a_\tau. \tag{38}$$

We have checked that in the mass region (32) all the coefficients $c_i > 0$. The parameter β is defined in (15). We plotted the corresponding exclusion curve in Fig. 4 labeled by (b) for the case of the Majorana sterile neutrino. As seen, our limits are more stringent than the existing ones from CHARM [39] and DELPHI [41] experiments in the sterile neutrino mass region 300 MeV $\leq m_N \leq$ 900 MeV. Note that in difference from the existing limits on $|U_{\tau N}|$ our limits are model independent in the sense that we have not made any assumptions on the other two mixing parameters $|U_{eN}|$ and $|U_{\mu N}|$. Instead, we excluded them combining the experimental limits on the branching ratios of different processes (19), (20), and (29)–(31).

C. Sterile neutrino in the final state

Other experimental data which we apply for deriving limits on $U_{\tau N}$ are [38]

$$\mathrm{Br}(\tau^- \to l\bar{\nu}_l\nu_\tau) = (17.85[17.36] \pm 0.05)\%, \tag{39}$$

$$\mathrm{Br}(\tau^- \to \pi^-\nu_\tau) = (10.91 \pm 0.07)\%, \tag{40}$$

where in the first line the central value 17.85 corresponds to $l = e$ and 17.36 to $l = \mu$. Both these experimental results agree with the SM predictions within the standard deviations $\Delta^{\mathrm{exp}}(\tau \to l\nu\nu) = 0.05\%$ and $\Delta^{\mathrm{exp}}(\tau \to l\pi\nu) = 0.07\%$. We already commented in Sec. III A (after Eqs. (19) and (20)), that in the reported experimental results like in Eqs. (19), (20), (39), and (40) the final state neutrino assignment $\nu_{e,\mu,\tau}$ is made according to what is suggested by the SM. However, in the experiments, measuring these decays, the final state neutrinos cannot be actually identified and are observed as a missing energy signature. Therefore, it is liable to imagine that instead of one or even both of the standard light neutrinos in the final states of decay in (39) and (40) there may occur some other neutral particles such as sterile neutrinos. We assume that in these modes of τ decay appears one sterile neutrino N accompanied by any of ν_e, ν_μ, ν_τ. Its mass must satisfy to $m_N \leq m_\tau - m_l$ and $m_N \leq m_\tau - m_\pi$ for the decays (39) and (40) respectively. We also assume that this contribution, if it exists, should be less than the corresponding standard deviation Δ^{exp}.

The contribution of sterile neutrino N to (39) and (40) in the form

$$\tau^- \to l\bar{\nu}_l N, \qquad \tau^- \to \pi^- N, \tag{41}$$

should be less than the corresponding Δ^{exp} since (39) and (40) are in agreement with the SM.

Therefore, using (A2) and (A3) we find the limits

$$|U_{\tau N}|^2 \leq \mathrm{Min}\left\{\frac{\Delta^{\mathrm{exp}}(\tau^- \to \pi^-\nu)}{\Gamma_\tau^{(\pi N)}}, \frac{\Delta^{\mathrm{exp}}(\tau^- \to \nu\nu l^-)}{\Gamma_\tau^{(N\nu l)}}\right\}, \tag{42}$$

where the minimal of the two values in the curly braces are selected for each value of m_N. The corresponding exclusion curve is shown in Fig. 4 and comprises the two parts (c) and (e). Part (c) is dominated by the constraints on purely leptonic τ decay mode while part (e) is mainly due to the semileptonic mode shown in (41). The exclusion curve (c), (e) cover a mass region $0 \leq m_N \leq m_\tau - m_\pi \approx$ 1640 MeV. This curve sets new limits on $U_{\tau N}$ for $0 \leq m_N \leq 70$ MeV and 300 MeV $\leq m_N \leq 700$ MeV. In the region 500 MeV $\leq m_N \leq 700$ MeV they are less stringent than our limits derived in the previous subsection from the data (19), (20), and (29)–(31) and corresponding to curve (b) in Fig. 4. For $m_N \leq 100$ MeV part (c) of our exclusion curve is nearly constant and our limits for this mass range can be displayed as

$$|U_{\tau N}|^2 \leq 2.9 \times 10^{-3}, \quad \text{for } 0 \leq m_N \leq 100 \text{ MeV}. \tag{43}$$

As we discussed previously, the sterile neutrino produced in (41) can decay within a detector with a probability P_N defined in (17). This would result in the appearance of a displaced vertex attributed to this sort of decay in addition to the production vertex (41). The limit in (42) does not take into account such a possibility and sums up the event rates of sterile neutrino decay both within and outside a detector. However, one can imagine an experiment where the displaced vertices of the above mentioned type are looked for and are either observed or, more probably, excluded at certain confidence level. For the latter case our limits in the region $m_N > 100$ MeV would drastically change. In order to illustrate the influence of this additional criterium of event selection on our limits we impose on the processes (41), a condition that the sterile neutrino decays outside the detector. This results in multiplication of the corresponding decay rate formulas (A2) and (A3) by the probability factor $1 - P_N$. The modified limits take the form

$$|U_{\tau N}|^2 \leq \mathrm{Min}\left\{\frac{\Delta^{\mathrm{exp}}(\tau^- \to \pi^-\nu)}{\Gamma_\tau^{(\pi N)}}, \frac{\Delta^{\mathrm{exp}}(\tau^- \to \nu\nu l^-)}{\Gamma_\tau^{(N\nu l)}}\right\} \times \exp(L_D\Gamma_N^0). \tag{44}$$

Here we used an inequality $\exp(L_D\Gamma_N) \leq \exp(L_D\Gamma_N^0)$, where $\Gamma_N^0 = a_e(m_N) + a_\mu(m_N) + a_\tau(m_N)$ with $a_{e,\mu,\tau}$ defined in (A17) and (A18). In this case our exclusion curve for $|U_{\tau N}|^2$ in Fig. 4 in comparison to the case of (42) changes its part (e) to (d) leaving part (c) intact. Now the exclusion curve (c)–(d) covers a mass region $0 \leq m_N \leq m_\tau - m_\pi \approx 180$ MeV. Note again that this is just an

illustration of an impact of as yet nonexisting experimental data allowing discrimination of the events with the displaced vertices associated with the sterile neutrino decay.

IV. SUMMARY AND CONCLUSIONS

We studied the resonant contribution of the sterile neutrino to leptonic and semileptonic decays of τ as well as to some semileptonic decays of K and D mesons. Comparison of our predictions with the corresponding experimental data on these decays allowed us to extract new limits on the mixing matrix element $U_{\tau N}$ shown in Fig. 4 as curves (b), (c), (e). In the two domains of the sterile neutrino mass $0 \leq m_N \leq 70$ MeV and 300 MeV $\leq m_N \leq$ 900 MeV our limits on $U_{\tau N}$ are more stringent than the limits existing in the literature. For $0 \leq m_N \leq 100$ MeV our limit to a good approximation is $|U_{\tau N}|^2 \leq 2.9 \times 10^{-3}$.

We also obtained new, although not stringent, limits on the products $|U_{\tau N} U_{eN}|$ and $|U_{\tau N} U_{\mu N}|$ shown in Figs. 5 and 6. To the best of our knowledge, limits on these products of the mixing matrix elements for $m_N \leq 100$ MeV do not exist in the literature.

Our limits derived from the experimental results (39) and (40) are, to a certain extent, conservative estimates. In fact, let us assume that in the derivation of these experimental values specific kinematical criteria for event selection were applied, suppressing the possible contribution of $\tau \to \pi N$, $l\nu N$ decays with a massive neutral particle N, such as a sterile neutrino, instead of the nearly massless neutrino. Then, taking these criteria in derivation of limits on $|U_{\tau N}|$ properly into account would have to strengthen them in comparison with our limits in Fig. 4. This sort of analysis is beyond the scope of the present paper and requires many additional and unknown details on the derivation of (39) and (40) carried out by the corresponding experimental groups.

We consider, as an important point of our analysis, its model independent character in the sense that we do not refer to any sort of *ad hoc* assumptions about the other two mixing matrix elements U_{eN} and $U_{\mu N}$. Such assumptions are typical for the existing literature on this subject. In particular, the limits of the CHARM [39] and NOMAD [40] collaborations shown in Fig. 4 were obtained under the assumption $|U_{\tau N}| \gg |U_{\mu N}|, |U_{eN}|$. At first, this assumption looks reasonable since the existing limits on $|U_{\mu N}|$ and $|U_{eN}|$ are very stringent (cf. Ref. [28]). However, they were also obtained under the assumptions of this type. To our mind these observations should be taken into account in assessment of the limits on the sterile neutrino mixing matrix elements $U_{\alpha N}$. In some cases these limits may be rather stringent mainly because of this sort of assumption.

ACKNOWLEDGMENTS

We thank S. Kuleshov, W. Brooks and C. Dib for useful discussions. This work was supported by FONDECYT Project No. 1100582, 110287, CONICYT(Chile) under Project No. 791100017 and Centro-Científico-Tecnológico de Valparaíso Project No. PBCT ACT-028.

APPENDIX: PARTIAL DECAY RATES

Here we specify the partial decay rates involved in Eqs. (7)–(12). For more details and discussion we refer the reader to Refs. [2,25,28]

The decay rates of mesons and τ to the final states with sterile neutrino N:

$$\Gamma(M^+ \to l_i^+ N) = |U_{iN}|^2 \frac{G_F^2}{8\pi} f_M^2 |V_M|^2 m_M^3 \lambda^{(1/2)}(x_i^2, x_N^2, 1)(x_i^2 + x_N^2 - (x_i^2 - x_N^2)^2) \equiv |U_{iN}|^2 \Gamma_M^{(l_i N)}, \tag{A1}$$

$$\Gamma(\tau^- \to \pi^- N) = |U_{\tau N}|^2 \frac{G_F^2}{16\pi} m_\tau^3 f_\pi^2 |V_{ud}|^2 F_P(z_N, z_P) \equiv |U_{\tau N}|^2 \Gamma_\tau^{(\pi N)}, \tag{A2}$$

$$\Gamma(\tau^- \to l^- \nu_l N) = |U_{\tau N}|^2 \frac{G_F^2}{192\pi^3} m_\tau^5 I_1(z_N, z_{\nu_l}, z_l) \equiv |U_{\tau N}|^2 \Gamma_\tau^{(l\nu N)}, \tag{A3}$$

$$\Gamma(\tau^- \to l^- \nu_\tau N) = |U_{lN}|^2 \frac{G_F^2}{192\pi^3} m_\tau^5 I_1(z_N, z_{\nu_\tau}, z_l) \equiv |U_{lN}|^2 \Gamma_\tau^{(l\nu N)}. \tag{A4}$$

Here we denoted $z_i = m_i/m_\tau$, $x_i = m_i/m_M$ with $m_i = m_N$, m_P, m_l. The kinematical functions $F_P(x, y)$, $I_1(x, y, z)$ are defined in (A13).

The partial decay rates of the heavy sterile neutrino, N including leptonic and semileptonic decay modes. In the latter case the final hadronic states for low neutrino masses $m_N < m_\rho$ is represented by the lightest mesons while for larger $m_N > m_\rho$ by $q\bar{q}$ pairs as suggested by the Bloom-Gilman duality [42]. This inclusive approach [2] allows one to reduce uncertainties in the leptonic decay constants f_M of mesons starting from the ρ meson, some of which are only known in phenomenological models (for more details see Ref. [2]). The list of the sterile neutrino decay rates is as follows:

$$\Gamma(N \to l_1^- l_2^+ \nu_{l_2}) = |U_{l_1 N}|^2 \frac{G_F^2}{192\pi^3} m_N^5 I_1(y_{l_1}, y_{\nu_{l_2}}, y_{l_2})(1 - \delta_{l_1 l_2}) \equiv |U_{l_1 N}|^2 \Gamma^{(l_1 l_2 \nu)}, \tag{A5}$$

$$\Gamma(N \to \nu_{l_1} l_2^- l_2^+) = |U_{l_1 N}|^2 \frac{G_F^2}{96\pi^3} m_N^5 [(g_L^l g_R^l + \delta_{l_1 l_2} g_R^l) I_2(y_{\nu_{l_1}}, y_{l_2}, y_{l_2}) + ((g_L^l)^2 + (g_R^l)^2 + \delta_{l_1 l_2}(1 + 2g_L^l)) I_1(y_{\nu_{l_1}}, y_{l_2}, y_{l_2})] \equiv |U_{l_1 N}|^2 \Gamma^{(l_2 l_2 \nu)}, \tag{A6}$$

$$\sum_{l_2 = e,\mu,\tau} \Gamma(N \to \nu_{l_1} \nu_{l_2} \bar{\nu}_{l_2}) = |U_{l_1 N}|^2 \frac{G_F^2}{96\pi^3} m_N^5 \equiv |U_{l_1 N}|^2 \Gamma^{(3\nu)}, \tag{A7}$$

$$\Gamma(N \to l_1^- P^+) = |U_{l_1 N}|^2 \frac{G_F^2}{16\pi} m_N^3 f_P^2 |V_P|^2 F_P(y_{l_1}, y_P) \equiv |U_{l_1 N}|^2 \Gamma^{(lP)}, \tag{A8}$$

$$\Gamma(N \to \nu_{l_1} P^0) = |U_{l_1 N}|^2 \frac{G_F^2}{64\pi} m_N^3 f_P^2 (1 - y_P^2)^2 \equiv |U_{l_1 N}|^2 \Gamma^{(\nu P)}, \tag{A9}$$

$$\Gamma(N \to l_1^- u \bar{d}) = |U_{l_1 N}|^2 |V_{ud}^{\mathrm{CKM}}|^2 \frac{G_F^2}{64\pi^3} m_N^5 I_1(y_{l_1}, y_u, y_d) \equiv |U_{l_1 N}|^2 \Gamma^{(lud)}, \tag{A10}$$

$$\Gamma(N \to \nu_{l_1} q \bar{q}) = |U_{l_1 N}|^2 \frac{G_F^2}{32\pi^3} m_N^5 [g_L^l g_R^l I_2(y_{\nu_{l_1}}, y_q, y_q) + ((g_L^l)^2 + (g_R^l)^2)) I_1(y_{\nu_{l_1}}, y_q, y_q)] \equiv |U_{l_1 N}|^2 \Gamma^{(\nu q q)}. \tag{A11}$$

Here $P = \pi, K$. The decay constants are $f_\pi = 130$ MeV, $f_K = 159$ MeV. We denoted $y_i = m_i/m_N$ with $m_i = m_l$, m_P, m_q. The Cabibbo-Kobayashi-Maskawa quark-mixing matrix (CKM) factors in Eq. (A8) are $V_\pi = V_{ud}^{\mathrm{CKM}}$, $V_K = V_{us}^{\mathrm{CKM}}$. For the quark masses we use the values $m_u \approx m_d = 3.5$ MeV, $m_s = 105$ MeV, $m_c = 1.27$ GeV, $m_b = 4.2$ GeV. In Eqs. (A10) and (A11) we denoted $u = u, c, t$; $d = d, s, b$ and $q = u, d, c, s, b, t$. The SM neutral current couplings of leptons and quarks are

$$g_L^l = -1/2 + \sin^2\theta_W, \qquad g_L^u = 1/2 - (2/3)\sin^2\theta_W,$$
$$g_L^d = -1/2 + (1/3)\sin^2\theta_W, \qquad g_R^l = \sin^2\theta_W, \tag{A12}$$
$$g_R^u = -(2/3)\sin^2\theta_W, \qquad g_R^d = (1/3)\sin^2\theta_W.$$

The kinematical functions in Eqs. (A1)–(A11) are

$$I_1(x, y, z) = 12 \int_{(x+y)^2}^{(1-z)^2} \frac{ds}{s}(s - x^2 - y^2)(1 + z^2 - s) \times \lambda^{1/2}(s, x^2, y^2)\lambda^{1/2}(1, s, z^2), \tag{A13}$$

$$I_2(x, y, z) = 24yz \int_{(y+z)^2}^{(1-x)^2} \frac{ds}{s}(1 + x^2 - s) \times \lambda^{1/2}(s, y^2, z^2)\lambda^{1/2}(1, s, x^2), \tag{A14}$$

$$F_P(x, y) = \lambda^{1/2}(1, x^2, y^2)[(1 + x^2)(1 + x^2 - y^2) - 4x^2]. \tag{A15}$$

The total decay rate Γ_N of the heavy neutrino N is equal to the sum of the partial decay rates in Eqs. (A5)–(A11), which we write in the form:

$$\Gamma_N = \sum_{l_1, l_2, \mathcal{H}} (1 + \delta_N)[\Gamma(N \to l_1^- \mathcal{H}^+) + \Gamma(N \to l_1^- l_2^+ \nu_{l_2}) + \Gamma(N \to \nu_{l_1} \mathcal{H}^0) + \Gamma(N \to l_2^- l_2^+ \nu_{l_1}) + \Gamma(N \to \nu_{l_1} \nu_{l_2} \bar{\nu}_{l_2})], \tag{A16}$$

where we denoted the hadronic states $\mathcal{H}^+ = P^+, \bar{d}u, \bar{s}u, \bar{d}c, \bar{s}c$ and $\mathcal{H}^0 = P^0, \bar{q}q$. We introduced the factor $\delta_N = 1$ for Majorana and $\delta_N = 0$ for Dirac neutrino N. Its appearance is related with the fact that for Majorana neutrinos both charge conjugate final states are allowed: $N \to l_1^- l_2^+ \nu_{l_2}$, $l_1^+ l_2^- \bar{\nu}_{l_2}$; $N \to l_2^- l_2^+ \nu_{l_1}$, $l_2^+ l_2^- \bar{\nu}_{l_1}$ and $N \to l^\mp \mathcal{H}^\pm$. For convenience we write Eq. (A16) in the form:

$$\Gamma_N = a_e(m_N) \cdot |U_{eN}|^2 + a_\mu(m_N) \cdot |U_{\mu N}|^2 + a_\tau(m_N) \cdot |U_{\tau N}|^2, \tag{A17}$$

where

$$a_l(m_N) = (1 + \delta_N)\left[\Gamma^{(l\mathcal{H})} + \Gamma^{(3\nu)} + \sum_{l_2}(\Gamma^{(l_2 l_2 \nu)} + \Gamma^{(l l_2 \nu)})\right], \tag{A18}$$

with $l, l_2 = e, \mu, \tau$. In the inclusive approach the hadronic contribution is calculated as

$$\Gamma^{(l\mathcal{H})} = \theta(\mu_0 - m_N) \sum_{P=\pi,K} (\Gamma^{(\nu P)} + \Gamma^{(lP)}) + \theta(m_N - \mu_0) \sum_{u,d,q} (\Gamma^{(lud)} + \Gamma^{(\nu q q)}). \tag{A19}$$

The parameter μ_0 denotes the mass threshold from which we start taking into account hadronic contributions via $q\bar{q}$ production. In Refs. [2,25] we have shown that the reasonable choice is $\mu_0 = m_{\rho^+} = 775.8$ MeV, which we also use in the analysis of the present paper. In Fig. 2 we plotted $\Gamma_{N0} \equiv \Gamma_N(U_{eN} = U_{\mu N} = U_{\tau N} = 1)$ as a function of the sterile neutrino mass m_N.

[1] J. Schechter and J. W. F. Valle, Phys. Rev. D **22**, 2227 (1980).

[2] V. Gribanov, S. Kovalenko, and I. Schmidt, Nucl. Phys. **B607**, 355 (2001).

[3] M. C. Gonzalez-Garcia and M. Maltoni, Phys. Rep. **460**, 1 (2008).

[4] P. Minkowski, Phys. Lett. B **67**, 421 (1977); T. Yanagida, in *Proc. of the Workshop on Grand Unified Theory and Baryon Number of the Universe* (KEK, Japan, 1979); M. Gell-Mann, P. Ramond, and R. Slansky, Sanibel Symposium Report No. CALT-68-709, 1979 (unpublished), http://arxiv.org/PS_cache/hep-ph/pdf/9809/9809459v1.pdf; and in *Supergravity*, edited by D. Freedman *et al.* (North Holland, Amsterdam, 1979); S. L. Glashow, in *Quarks and Leptons*, edited by Cargese, M. Levy *et al.* (Plenum, New York, 1980), p. 707; R. N. Mohapatra and G. Senjanovic, Phys. Rev. Lett. **44**, 912 (1980).

[5] F. del Aguila, J. A. Aguilar-Saavedra, J. de Blas, and M. Zralek, Acta Phys. Pol. B **38**, 3339 (2007), http://th-www.if.uj.edu.pl/acta/vol38/pdf/v38p3339.pdf; X. G. He, S. Oh, J. Tandean, and C. C. Wen, Phys. Rev. D **80**, 073012 (2009); W. Buchmuller and C. Greub, Nucl. Phys. **B363**, 345 (1991); G. Ingelman and J. Rathsman, Z. Phys. C **60**, 243 (1993); F. del Aguila, J. A. Aguilar-Saavedra, A. Martinez de la Ossa, and D. Meloni, Phys. Lett. B **613**, 170 (2005); A. Pilaftsis and T. E. J. Underwood, Phys. Rev. D **72**, 113001 (2005); J. Kersten and A. Y. Smirnov, Phys. Rev. D **76**, 073005 (2007); A. Ibarra, E. Molinaro, and S. T. Petcov, J. High Energy Phys. 09 (2010) 108.

[6] J. A. Harvey, P. Ramond, and D. B. Reiss, Nucl. Phys. **B199**, 223 (1982); S. Dimopoulos, L. J. Hall, and S. Raby, Phys. Rev. Lett. **68**, 1984 (1992); L. J. Hall and S. Raby, Phys. Rev. D **51**, 6524 (1995).

[7] I. Dorsner and P. Fileviez Pérez, Nucl. Phys. **B723**, 53 (2005); I. Dorsner, P. Fileviez Pérez, and R. Gonzalez Felipe, Nucl. Phys. **B747**, 312 (2006); P. Fileviez Pérez, AIP Conf. Proc. **903**, 385 (2007); I. Dorsner, P. Fileviez Pérez, and G. Rodrigo, Phys. Rev. D **75**, 125007 (2007).

[8] J. Schechter and J. W. F. Valle, Phys. Rev. D **25**, 774 (1982).

[9] J. Hisano, T. Moroi, K. Tobe, and M. Yamaguchi, Phys. Rev. D **53**, 2442 (1996); J. R. Ellis, J. Hisano, M. Raidal, and Y. Shimizu, Phys. Rev. D **66**, 115013 (2002); F. Deppisch, H. Paes, A. Redelbach, R. Rückl, and Y. Shimizu, Eur. Phys. J. C **28**, 365 (2003); S. T. Petcov, S. Profumo, Y. Takanishi, and C. E. Yaguna, Nucl. Phys. **B676**, 453 (2004); E. Arganda and M. J. Herrero, Phys. Rev. D **73**, 055003 (2006); S. T. Petcov, T. Shindou, and Y. Takanishi, Nucl. Phys. **B738**, 219 (2006); S. Antusch, E. Arganda, M. J. Herrero, and A. M. Teixeira, J. High Energy Phys. 11 (2006) 090; F. Deppisch and J. W. F. Valle, Phys. Rev. D **72**, 036001 (2005); J. Hisano, T. Moroi, K. Tobe, M. Yamaguchi, and T. Yanagida, Phys. Lett. B **357**, 579 (1995); E. Arganda, M. J. Herrero, and A. M. Teixeira, J. High Energy Phys. 10 (2007) 104; J. N. Esteves, J. C. Romao, M. Hirsch, F. Staub, and W. Porod, Phys. Rev. D **83**, 013003 (2011); M. Hirsch, T. Kernreiter, J. C. Romao, and A. Villanova del Moral, J. High Energy Phys. 01 (2010) 103; J. N. Esteves, S. Kaneko, J. C. Romao, M. Hirsch, and W. Porod, Phys. Rev. D **80**, 095003 (2009); J. N. Esteves, J. C. Romao, A. Villanova del Moral, M. Hirsch, J. W. F. Valle, and W. Porod, J. High Energy Phys. 05 (2009) 003; M. Hirsch, S. Kaneko, and W. Porod, Phys. Rev. D **78**, 093004 (2008); M. Hirsch, J. W. F. Valle, W. Porod, J. C. Romao, and A. Villanova del Moral, Phys. Rev. D **78**, 013006 (2008).

[10] See, for example, R. N. Mohapatra and P. B. Pal, *Massive Neutrinos in Physics and Astrophysics* (World Scientific, Singapore, 1991).

[11] I. Dorsner and P. Fileviez Perez, J. High Energy Phys. 06 (2007) 029; B. Bajc, M. Nemevsek, and G. Senjanovic, Phys. Rev. D **76**, 055011 (2007).

[12] A. de Gouvea, J. Jenkins, and N. Vasudevan, Phys. Rev. D **75**, 013003 (2007).

[13] M. Viel, J. Lesgourgues, M. G. Haehnelt, S. Matarrese, and A. Riotto, Phys. Rev. D **71**, 063534 (2005); Phys. Rev. Lett. **97**, 071301 (2006).

[14] G. M. Fuller, A. Kusenko, and K. Petraki, Phys. Lett. B **670**, 281 (2009).

[15] S. Dodelson and L. M. Widrow, Phys. Rev. Lett. **72**, 17 (1994); X. D. Shi and G. M. Fuller, Phys. Rev. Lett. **82**, 2832 (1999); A. D. Dolgov and S. H. Hansen, Astropart. Phys. **16**, 339 (2002).

[16] K. Abazajian, G. M. Fuller, and M. Patel, Phys. Rev. D **64**, 023501 (2001).

[17] G. Gelmini, S. Palomares-Ruiz, and S. Pascoli, Phys. Rev. Lett. **93**, 081302 (2004).

[18] T. Asaka, S. Blanchet, and M. Shaposhnikov, Phys. Lett. B **631**, 151 (2005); T. Asaka and M. Shaposhnikov, Phys. Lett. B **620**, 17 (2005); T. Asaka, M. Laine, and M. Shaposhnikov, J. High Energy Phys. 01 (2007) 091; T. Asaka, M. Shaposhnikov, and A. Kusenko, Phys. Lett. B **638**, 401 (2006).

[19] K. Abazajian, G. M. Fuller, and W. H. Tucker, Astrophys. J. **562**, 593 (2001); A. Boyarsky, A. Neronov, O. Ruchayskiy, and M. Shaposhnikov, Phys. Rev. D **74**, 103506 (2006); A. Boyarsky, A. Neronov, O. Ruchayskiy, M. Shaposhnikov, and I. Tkachev, Phys. Rev. Lett. **97**, 261302 (2006).

[20] A. D. Dolgov, Phys. Rep. **370**, 333 (2002).

[21] A. Y. Smirnov and R. Zukanovich Funchal, Phys. Rev. D **74**, 013001 (2006).

[22] A. Kusenko, Phys. Rep. **481**, 1 (2009).

[23] R. E. Shrock, Phys. Lett. B **96**, 159 (1980).

[24] C. Dib, V. Gribanov, S. Kovalenko, and I. Schmidt, Phys. Lett. B **493**, 82 (2000).

[25] J. C. Helo, Sergey Kovalenko, and Ivan Schmidt, Nucl. Phys. **B853**, 80 (2011).

[26] G. Cvetic, C. Dib, S. K. Kang, and C. S. Kim, Phys. Rev. D **82**, 053010 (2010).

[27] M. A. Ivanov and S. G. Kovalenko, Phys. Rev. D **71**, 053004 (2005).

[28] A. Atre, T. Han, S. Pascoli, and B. Zhang, J. High Energy Phys. 05 (2009) 030.

[29] F. M. L. Almeida, Y. A. Coutinho, J. A. Martins Simoes, and M. A. B. do Vale, Phys. Rev. D **62**, 075004 (2000).

[30] O. Panella, M. Cannoni, C. Carimalo, and Y. N. Srivastava, Phys. Rev. D **65**, 035005 (2002).

[31] T. Han and B. Zhang, Phys. Rev. Lett. **97**, 171804 (2006).

[32] S. Kovalenko, Z. Lu, and I. Schmidt, Phys. Rev. D **80**, 073014 (2009).

[33] G. Cvetic, C. Dib, C. S. Kim, and J. D. Kim, Phys. Rev. D **74**, 093011 (2006).
[34] A. Kusenko, S. Pascoli, and D. Semikoz, J. High Energy Phys. 11 (2005) 028.
[35] A. Aguilar *et al.*, Phys. Rev. D **64**, 112007 (2001), and references therein.
[36] A. A. Aguilar-Arevalo *et al.*, Phys. Rev. Lett. **105**, 181801 (2010).
[37] S. N. Gninenko, Phys. Rev. Lett. **103**, 241802 (2009); Phys. Rev. D **83**, 015015 (2011); **83**, 093010 (2011); S. N. Gninenko and D. S. Gorbunov, Phys. Rev. D **81**, 075013 (2010).
[38] K. Nakamura *et al.* (Particle Data Group), J. Phys. G **37**, 075021 (2010).
[39] J. Orloff, A. N. Rozanov, and C. Santoni, Phys. Lett. B **550**, 8 (2002).
[40] P. Astier *et al.* (NOMAD Collaboration), Phys. Lett. B **506**, 27 (2001).
[41] P. Abreu *et al.* (DELPHI Collaboration), Z. Phys. C **74**, 57 (1997); **75**, 580(E) (1997), http://www.springerlink.com/content/gqugwjxet2jl79qf/;
[42] E. D. Bloom and F. J. Gilman, Phys. Rev. Lett. **25**, 1140 (1970); Phys. Rev. D **4**, 2901 (1971).